Pergamon

PII: S0277-5387(97)00290-8

Polyhedron Vol. 17, No. 5–6, pp. 857–867, 1998

0277-5387/98 $19.00+0.00

Pyridine, isocyanide, carbodiimide and allene adducts of hexakis(trifluoromethyl *t*-botoxy)ditungsten. A comparison of ligand binding to $W_2(O^tBu)_6$ and $W_2(OCMe_2CF_3)_6$†

Theodore A. Budzichowski, M. H. Chisholm,* Kristen Folting,
John C. Huffman, William E. Streib and Darin B. Tiedtke

Department of Chemistry and Molecular Structure Center, Indiana University, Bloomington,
IN 47405, U.S.A.

(Received 2 May 1997; accepted 23 June 1997)

Abstract—$W_2(OR)_6$ compounds, where R = ^{t}Bu and CMe_2CF_3, both reversibly bind pyridine in hydrocarbon solvents to form adducts $W_2(OR)_6L_2$. Pyridine binds more strongly to the fluoroalkoxide but the structural parameters of the compounds $W_2(OCMe_2CF_3)_6(C_6H_5N)_2$ and $W_2(O^tBu)_6(4\text{-}CH_3C_6H_4N)_2$ reveal an essentially identical $W_2O_6N_2$ core with W—W = 2.39(1) Å, W—O = 1.92–1.95 Å and W—N = 2.26(1) Å. Both compounds were crystallographically characterized in the space group *C*2/*c* and each molecule has rigorous C_2 symmetry. Allene and 1,3-di-*p*-tolylcarbodiimide form 1 : 1 adducts with $W_2(OCMe_2CF_3)_6$ in which the substrate is bound parallel to the M-M axis, i.e. $\mu\text{-}\eta^2,\eta^2\text{-}C_3H_4$ and $\mu\text{-}\eta^2,\eta^2$-ArNCNAr-$W_2(OCMe_2CF_3)_6$. Also $W_2(OCMe_2CF_3)_6$ and $W_2(OSi^tBuMe_2)_6$ bind two equivalents of xylylisocyanide to afford $W_2(OR)_6(\eta^1\text{-}CNAr)_2$. For $W_2(OCMe_2CF_3)_6(\eta^1\text{-}CNAr)_2$, the molecular structure has been determined by X-ray crystallography and shows a nearly eclipsed central $W_2O_6C_2$ skeleton with W—W = 2.44(1) Å, W—O = 1.94(1) Å (av.) and W—C = 2.14(1) Å, whereas the W—W—O angles span the range 105–114°, the W—W—C angles are 83(1)°. Similarly, $W_2(OCMe(CF_3)_2)_4(NMe_2)_2$ forms a *bis* adduct upon reaction with the isocyanide. However, the molecular structure of $W_2(OCMe(CF_3)_2)_4(NMe_2)_2(\eta^1\text{-}CNAr)_2$ shows a staggered arrangement of the two ligands about the ditungsten center where W—W = 2.382(1) Å, W—O = 2.00(1) Å (av.), W—N = 1.93(1) Å (av.) and W—C = 2.14(1) Å (av.) with a C—W—W—C dihedral angle of 41.9°. These reactions and their products are compared for $W_2(OR)_6$ compounds where R = ^{t}Bu, ^{t}BuMe$_2$Si and CMe_2CF_3. © 1998 Elsevier Science Ltd. All rights reserved

Keywords: tungsten; M-M triple bonds; alkoxides; isocyanide; carbodiimide; allene.

The reactivity of a metal center is greatly influenced by its attendant ligands and perhaps nowhere is this more apparent than in catalysis. In our studies of the reactivity of compounds containing $(M{\equiv}M)^{6+}$ bonds we find that the nature of the metal, Mo versus W, and the attendant ligand set greatly influence reactivity but in a way in which we do not yet fully understand. For example, $W_2(O^tBu)_6$ and NO react in the presence of pyridine (py) to give $W(O^tBu)_3(NO)(py)$ [1] by cleavage of the W—W triple bond whereas NO and $W_2(OSi^tBuMe_2)_6$ yield N_2 and oxotungsten siloxides [2]. $Mo_2(O^tBu)_6$ dissolves in acetonitrile whereas $W_2(O^tBu)_6$ and MeC≡N react virtually instantaneously at room temperature to give $({}^tBuO)_3W{\equiv}N$ and $({}^tBuO)_3W{\equiv}CMe$ [3]. $W_2(OCMe_2CF_3)_6$ and MeC≡N on the other hand react in solution to give an equilibrium wherein acetonitrile forms a σ- or η^1-N bound adduct, eq. (1) [4].

$$W_2(OCMe_2CF_3)_6 + 2MeC{\equiv}N \rightleftharpoons W_2(OCMe_2CF_3)_6(NCMe)_2 \quad (1)$$

While some of these remarkable differences in reactivity may be traced to thermodynamics, we are inclined to the view that kinetic factors are also important if not the dominant factors influencing reactivity

---

* Author to whom correspondence should be addressed.

† Dedicated to Professor D. C. Bradley, a life long friend and mentor.

[5]. Thus the frontier orbital energies of the substrates and metal centers involved are most significant. In this paper we compare further some reactivity studies of $W_2(OCMe_2CF_3)_6$, and other W_2^{6+} complexes supported by poorer π-donors, with the closely related compound $W_2(O^tBu)_6$.

RESULTS AND DISCUSSION

Syntheses and reactivity studies

Pyridine binds to both $W_2(O^tBu)_6$ and $W_2(OCMe_2CF_3)_6$ in hydrocarbon solutions. By ^1H NMR spectroscopy the binding is seen to be reversible according to eq. (2). The position of the equilibrium lies in favor of the binding to the trifluorobutoxide compound but an accurate measurement of K_{eq} has not been determined by these NMR studies. The equilibrium is dynamic on the NMR time-scale as is rotation about the M—M bond axis and for R = ^{t}Bu these are not frozen out until *ca* −30°C in toluene-d_8.

$$W_2(OR)_6+2py \rightleftharpoons W_2(OR)_6(py)_2 \qquad (2)$$

Crystals suitable for an X-ray study were obtained for $W_2(O^tBu)_6(4\text{-Me-py})_2$ from hexane and for $W_2(OCMe_2CF_3)_6(py)_2$ from benzene. Both compounds are dark brown, hydrocarbon-soluble, air-sensitive crystalline compounds.

Allene, $CH_2{=}C{=}CH_2$, and 1,3-di-*p*-tolylcarbodiimide form 1 : 1 adducts with $W_2(OCMe_2CF_3)_6$ while $W_2(OSi^tBuMe_2)_6$ is unreactive with these substrates. The new 1 : 1 adducts are green, hydrocarbon-soluble, air-sensitive crystalline compounds. Formation of these 1 : 1 adducts parallels the behavior of $W_2(O^tBu)_6$ [6]. However, the compound $W_2(O^tBu)_6(C_3H_4)$ is thermally unstable and, in solution, reacts to give the products derived from propyne, namely $W(O^tBu)_3(CMe)$ and $W(O^tBu)_3(CH)$ though that latter compound can only be detected in solution because it rapidly decomposes in the absence of a Lewis base such as py or quinuclidine [7]. Further reaction with allene gives the more thermally stable compound $W_2(O^tBu)_6(\mu\text{-}\eta^1,\eta^3\text{-}C_3H_4)(\eta^2\text{-}C_3H_4)$ [6a]. No such reactivity is observed for $W_2(OCMe_2CF_3)_6(C_3H_4)$, and the 1:1 adduct is unreactive in the presence of excess allene.

$W_2(OCMe_2CF_3)_6$, $W_2(OSi^tBuMe_2)_6$ and $W_2(OCMe(CF_3)_2)_4(NMe_2)_2$ react with aryl isocyanides to form bis adducts. For the fluoroalkoxide complexes, the xylylisocyanide adducts formed crystals suitable for X-ray studies. The coordination of the isocyanide ligand is evidently sufficiently strong that significant dissociation is not observed in solution at room temperature. The formation of the 2 : 1 adducts in the reactivity of these alkoxide supported W_2-complexes differs from the formation of the 1 : 1 adducts in the chemistry of $W_2(O^tBu)_6$. In the latter case, the isocyanide [8] and the carbonyl [9] form a bridge across the two metal atoms. The mixed amido-fluoroalkoxide compound $W_2(NMe_2)_2(OCMe(CF_3)_2)_6$ also forms a 2 : 1 adduct with xylylisocyanide and pyridine.

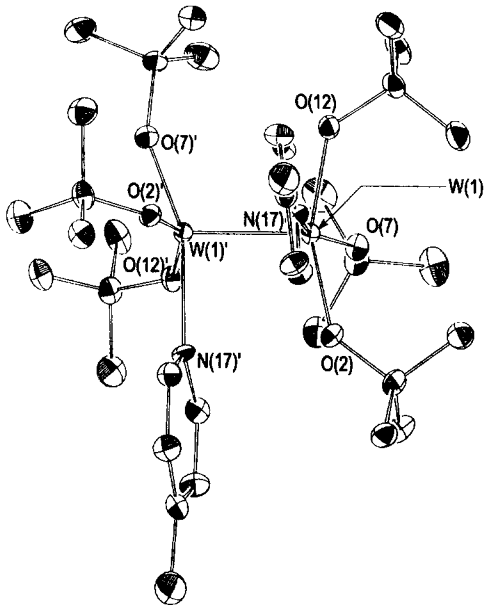

Fig. 1. An ORTEP drawing of the $W_2(O^tBu)_6(4\text{-Me-py})_2$ molecule.

NMR and other spectral characterization data are given in the Experimental Section.

Crystal and molecular structures

$W_2(O^tBu)_6(4\text{-Me-py})_2$ and $W_2(OCMe_2CF_3)_6(py)_2$ both crystallize in the space group *C2/c* with crys-

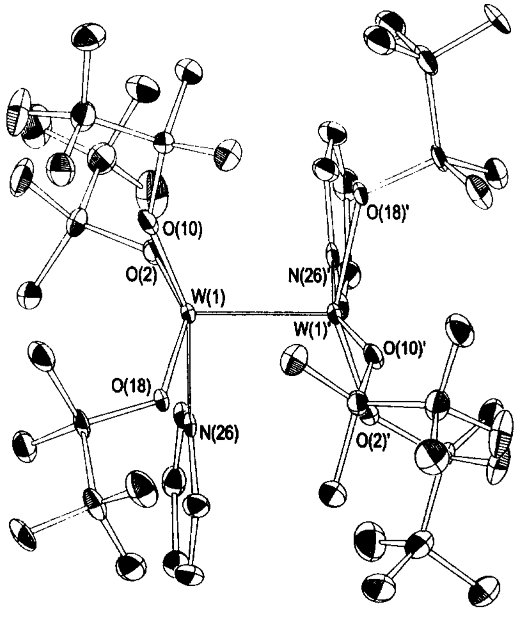

Fig. 2. An ORTEP drawing of the $W_2(OCMe_2CF_3)_6(py)_2$ molecule.

Table 1. Selected bond distances (Å) and angles (°) for $W_2(O^tBu)_6(4\text{-}Me\text{-}py)_2$

W(1)′—W(1)	2.397(1)
W(1)—O(2)	1.941(4)
W(1)—O(7)	1.930(4)
W(1)—O(12)	1.941(4)
W(1)—N(17)	2.254(5)
O(2)—C(3)	1.445(7)
O(7)—C(8)	1.420(7)
O(12)—C(13)	1.446(7)
W(1)′—W(1)—O(2)	103.5(1)
W(1)′—W(1)—O(7)	112.3(1)
W(1)′—W(1)—O(12)	100.6(1)
W(1)′—W(1)—N(17)	88.4(1)
O(2)—W(1)—O(7)	92.5(2)
O(2)—W(1)—O(12)	151.0(2)
O(2)—W(1)—N(17)	82.4(2)
O(7)—W(1)—O(12)	93.1(2)
O(7)—W(1)—N(17)	159.3(2)
O(12)—W(1)—N(17)	82.3(2)
W(1)—O(2)—C(3)	136.8(4)
W(1)—O(7)—C(8)	152.5(4)
W(1)—O(12)—C(13)	132.2(3)
W(1)—N(17)—C(18)	121.8(4)
W(1)—N(17)—C(22)	123.3(4)

tallographically imposed C_2 symmetry. ORTEP drawings of $W_2(O^tBu)_6(4\text{-}Me\text{-}py)_2$ and $W_2(OCMe_2(CF_3))_6(py)_2$ are given in Figs 1 and 2, respectively, and selected bond distances and bond angles are given in Tables 1 and 2. A view looking down the M—M axis for each molecule is given in Fig. 3.

The two molecules are seen to be remarkably similar in their solid-state structures. The W—W distances, 2.40(1) Å and the W—O distances, which range from 1.92 to 1.96 Å, are essentially identical within the 3σ criterion. Despite the more favorable binding of pyridine to $W_2(OCMe_2CF_3)_6$ this is not reflected in the W—N distances: 2.27(1) Å versus 2.25(1) Å for the 4-Me-pyridine ligand in $W_2(O^tBu)_6(4\text{-}Me\text{-}py)_2$. However, once again within the criterion of 3σ these W—N distances have to be viewed equivalent. Thus, the structures of the pyridine adducts offer no insight to the rather different reactivities of the two $W_2(OR)_6$ compounds.

$W_2(OCMe_2CF_3)_6(4\text{-}Me\text{-}C_6H_4CNCC_6H_4\text{-}4\text{-}Me)$ crystallized in the space group $P\bar{1}$ with a molecule of n-hexane at the crystallographic center of symmetry. The n-hexane was refined at 78% partial occupancy and the three carbon atoms in the asymmetric unit of this solvent molecule showed some disorder. Despite these problems the structure of the ditungsten complex was refined satisfactorily, at least with respect to

Table 2. Selected bond distances (Å) and angles (°) for $W_2(OCMe_2CF_3)_6(py)_2$

W(1)—W(1)′	2.3903(8)
W(1)—O(2)	1.954(5)
W(1)—O(10)	1.923(5)
W(1)—O(18)	1.958(5)
W(1)—N(26)	2.273(7)
C—F	1.34 (av.)
W(1)′—W(1)—O(2)	106.6(2)
W(1)′—W(1)—O(10)	109.4(2)
W(1)′—W(1)—O(18)	102.7(1)
W(1)′—W(1)—N(26)	89.3(2)
O(2)—W(1)—O(10)	93.2(2)
O(2)—W(1)—O(18)	146.5(2)
O(2)—W(1)—N(26)	81.9(2)
O(10)—W(1)—O(18)	92.1(2)
O(10)—W(1)—N(26)	161.2(2)
O(18)—W(1)—N(26)	82.6(2)
W(1)—O(2)—C(3)	136.2(5)
W(1)—O(10)—C(11)	148.3(5)
W(1)—O(18)—C(19)	127.2(5)
W(1)—N(26)—C(27)	122.0(5)
W(1)—N(26)—C(31)	121.6(5)

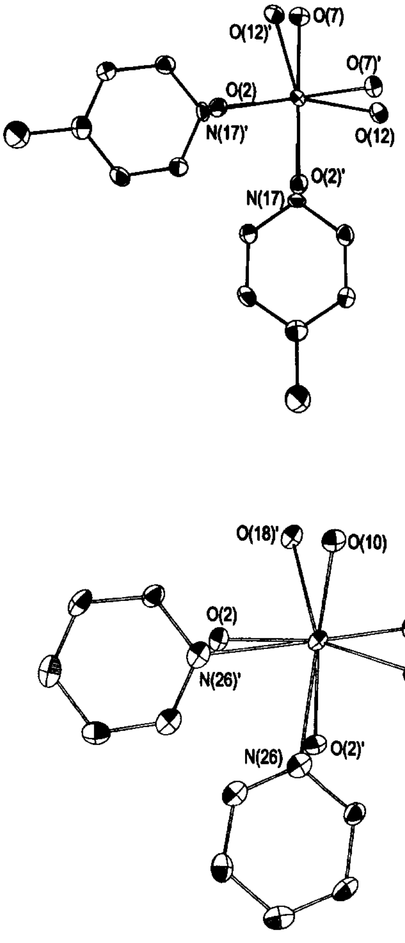

Fig. 3. Views of the central skeleton of the $W_2(O^tBu)_6(4\text{-}Me\text{-}py)_2$ and $W_2(OCMe_2CF_3)_6(py)_2$ molecules looking down the M—M—axis.

gross features of the molecular geometry. An ORTEP drawing of the molecule is given in Fig. 4. The bridging carbodiimide lies parallel to the M—M axis in a $\mu\eta^2,\eta^2$ manner. This imposes an eclipsed geometry for the O_3WWO_3 skeleton. Selected bond distances and bond angles are given in Table 3.

The W—W distance of 2.52 Å is the range expected for a $(W{=}W)^{8+}$ moiety consistent with the view that the carbodiimide is partially reduced. This is also reflected in the η^2-C—N distances of 1.28 Å and the N—C—N angle of 155°. The W—N distances, 2.08(1) Å (av.) and the W—C distances 2.19(1) Å (av.) also imply a strongly bound carbodiimide ligand. There is very little difference in the metrical parameters reported for $W_2(O^tBu)_6(\mu\eta^2,\eta^2$-ArNCNAr) by Cotton *et al.* [6b] with those found for the present structure.

$W_2(OCMe_2CF_3)_6(\mu$-$CH_2CCH_2)$. An ORTEP view of the molecule is given in Fig. 5 with selected bond distances and bond angles listed in Table 4. Superficially, the molecule is similar to the carbodiimide structure described previously but the W—W distance of 2.59 Å is significantly longer implying a greater degree of oxidation of the ditungsten center. Also the C—C—C angle of 141° deviates more from linearity than does the N—C—N angle. The C—C distances of 1.46 Å (av.) are comparable to Csp^2–Csp^2 single bond distances, certainly greatly reduced from those in free allene. The structure resembles in every way that of $W_2(O^tBu)_6(\mu\eta^2,\eta^2$-$C_3H_4)$ reported earlier [6a]. The W—O distances of the OR ligands trans to the W—C bonds are longer than those that are mutually trans implying that the allene ligand exerts a higher trans-influence [10] than the fluoroalkoxide.

$W_2(OCMe_2CF_3)_6$(CNxylyl)$_2$. An ORTEP drawing of the molecule is given in Fig. 6 and selected bond distances and bond angles are given in Table 5. The molecule has virtual but not crystallographically imposed C_2 symmetry. The W—W distance of 2.44(1) Å is longer than that expected for a triple bond but only slightly, c.f. the pyridine adducts described earlier. This can be understood in terms of the xylylisocyanide ligands acting as π-acceptor ligands. The central $W_2O_6C_2$ core is very similar to that seen for the $W_2(OCMe_2CF_3)_6(CO)_2$ molecule [11]. Note the

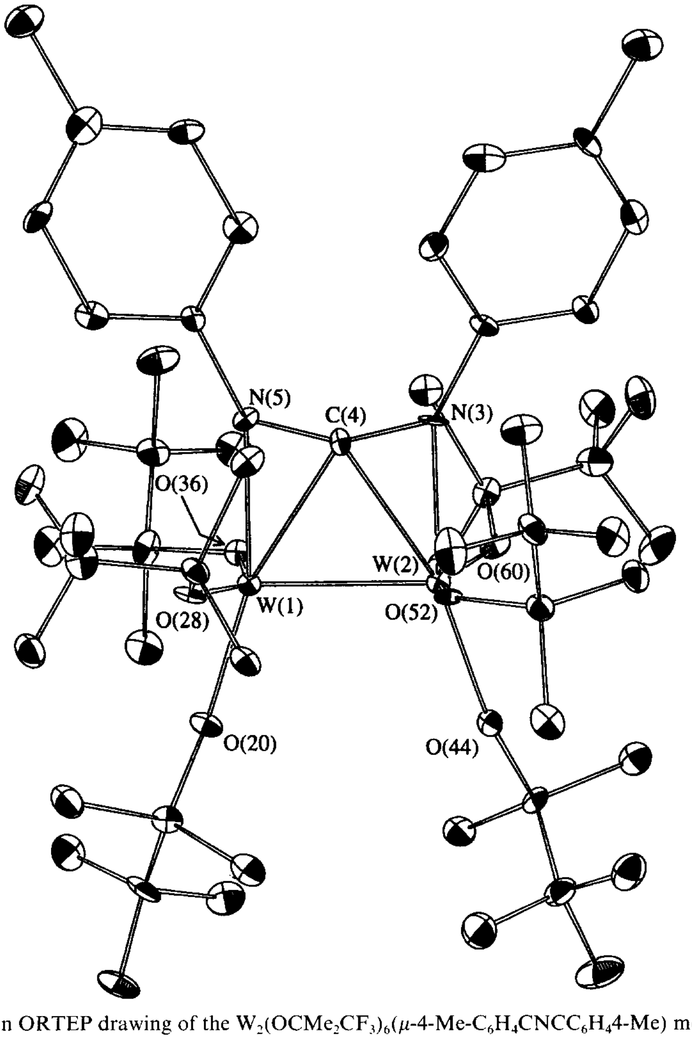

Fig. 4. An ORTEP drawing of the $W_2(OCMe_2CF_3)_6(\mu$-4-Me-$C_6H_4CNCC_6H_4$4-Me) molecule.

Table 3. Selected bond distances (Å) and angles (°) for $W_2(OCMe_2CF_3)_6(\mu\text{-}CH_2CCH_2)$

W(1)—W(2)	2.5930(6)
W(1)—O(6)	1.904(6)
W(1)—O(14)	1.936(6)
W(1)—O(22)	1.889(6)
W(1)—C(3)	2.118(9)
W(1)—C(4)	2.092(9)
W(2)—O(30)	1.889(6)
W(2)—O(38)	1.947(6)
W(2)—O(46)	1.898(6)
W(2)—C(4)	2.084(9)
W(2)—C(5)	2.144(9)
C—F	1.34(1) av.
C(3)—C(4)	1.464(12)
C(4)—C(5)	1.455(12)

W(2)—W(1)—O(6)	98.5(2)
W(2)—W(1)—O(14)	116.2(2)
W(2)—W(1)—O(22)	105.9(3)
W(2)—W(1)—C(3)	91.8(2)
W(2)—W(1)—C(4)	51.5(3)
O(6)—W(1)—O(14)	86.2(3)
O(6)—W(1)—O(22)	155.2(2)
O(6)—W(1)—C(3)	85.7(3)
O(6)—W(1)—C(4)	97.0(3)
O(14)—W(1)—O(22)	87.2(3)
O(14)—W(1)—C(3)	151.8(3)
O(14)—W(1)—C(4)	167.5(3)
O(22)—W(1)—C(3)	88.9(3)
O(22)—W(1)—C(4)	94.5(3)
C(3)—W(1)—C(4)	40.7(3)
W(1)—W(2)—O(30)	106.4(2)
W(1)—W(2)—O(38)	113.9(2)
W(1)—W(2)—O(46)	100.7(2)
W(1)—W(2)—C(4)	51.8(2)
W(1)—W(2)—C(5)	91.7(2)
O(30)—W(2)—O(38)	86.9(3)
O(30)—W(2)—O(46)	152.6(2)
O(30)—W(2)—C(4)	96.0(3)
O(30)—W(2)—C(5)	89.1(3)
O(38)—W(2)—O(46)	86.2(3)
O(38)—W(2)—C(4)	165.6(3)
O(38)—W(2)—C(5)	154.1(3)
O(46)—W(2)—C(4)	97.3(3)
O(46)—W(2)—C(5)	85.8(3)
C(4)—W(2)—C(5)	40.2(3)
W(1)—O(6)—C(7)	136.9(5)
W(1)—O(14)—C(15)	144.5(6)
W(1)—O(22)—C(23)	151.9(5)
W(2)—O(30)—C(31)	152.8(6)
W(2)—O(38)—C(39)	142.3(5)
W(2)—O(46)—C(47)	134.5(5)
W(1)—C(3)—C(4)	68.7(5)
W(1)—C(4)—W(2)	76.8(3)
W(1)—C(4)—C(3)	70.6(5)
W(1—C(4)—C(5)	148.0(7)
W(2)—C(4)—C(3)	145.9(7)
W(2)—C(4)—C(5)	72.1(5)
C(3)—C(4)—C(5)	141.3(8)
W(2)—C(5)—C(4)	67.7(5)

Table 4. Selected bond distances (Å) and angles (°) for $W_2(OCMe_2CF_3)_6(\mu\text{-}N(C\text{-}p\text{-}tolyl)_2)$

W(1)—W(2)	2.5064(8)
W(1)—O(20)	1.888(8)
W(1)—O(28)	1.949(8)
W(1)—O(36)	1.913(7)
W(1)—N(5)	2.088(9)
W(1)—C(4)	2.19(1)
W(2)—O(44)	1.891(8)
W(2)—O(52)	1.922(8)
W(2)—O(60)	1.950(7)
W(2)—N(3)	2.066(9)
W(2)—C(4)	2.19(1)
C—F	1.34(1) (av.)
N(3)—C(4)	1.28(2)
N(5)—C(4)	1.28(2)

W(2)—W(1)—O(20)	109.2(3)
W(2)—W(1)—O(28)	99.1(2)
W(2)—W(1)—O(36)	109.2(2)
W(2)—W(1)—N(5)	89.9(3)
W(2)—W(1)—C(4)	55.2(3)
O(20)—W(1)—O(28)	88.7(3)
O(20)—W(1)—O(36)	89.0(3)
O(20)—W(1)—N(5)	160.7(4)
O(20)—W(1)—C(4)	164.3(4)
O(28)—W(1)—O(36)	150.7(3)
O(28)—W(1)—N(5)	85.2(3)
O(28)—W(1)—C(4)	92.7(4)
O(36)—W(1)—N(5)	87.4(3)
O(36)—W(1)—C(4)	97.2(4)
N(5)—W(1)—C(4)	34.8(4)
W(1)—W(2)—O(44)	109.7(2)
W(1)—W(2)—O(52)	108.4(3)
W(1)—W(2)—O(60)	98.8(2)
W(1)—W(2)—N(3)	89.8(3)
W(1)—W(2)—C(4)	55.1(3)
O(44)—W(2)—O(52)	90.0(3)
O(44)—W(2)—O(60)	88.9(3)
O(44)—W(2)—N(3)	160.4(4)
O(44)—W(2)—C(4)	164.7(4)
O(52)—W(2)—O(60)	151.5(3)
O(52)—W(2)—N(3)	86.2(4)
O(52)—W(2)—C(4)	96.2(4)
O(60)—W(2)—N(3)	85.5(4)
O(60)—W(2)—C(4)	92.3(4)
N(3)—W(2)—C(4)	34.7(4)
W(1)—O(20)—C(21)	146.8(7)
W(1)—O(28)—C(29)	127.5(7)
W(1)—O(36)—C(37)	148.5(7)
W(2)—O(44)—C(45)	147.2(7)
W(2)—O(52)—C(53)	149.2(7)
W(2)—O(60)—C(61)	126.7(7)
W(2)—N(3)—C(4)	78.0(7)
W(2)—N(3)—C(6)	148.8(8)
C(4)—N(3)—C(6)	132.5(1)
W(1)—N(5)—C(4)	76.9(7)
W(1)—N(5)—C(13)	150.4(8)
C(4)—N(5)—C(13)	131.9(1)
W(1)—C(4)—W(2)	69.8(3)
W(1)—C(4)—N(3)	137.0(9)
W(1)—C(4)—N(5)	68.3(6)
W(2)—C(4)—N(3)	67.2(6)
W(2)—C(4)—N(5)	138.0(9)
N(3)—C(4)—N(5)	154.7(12)

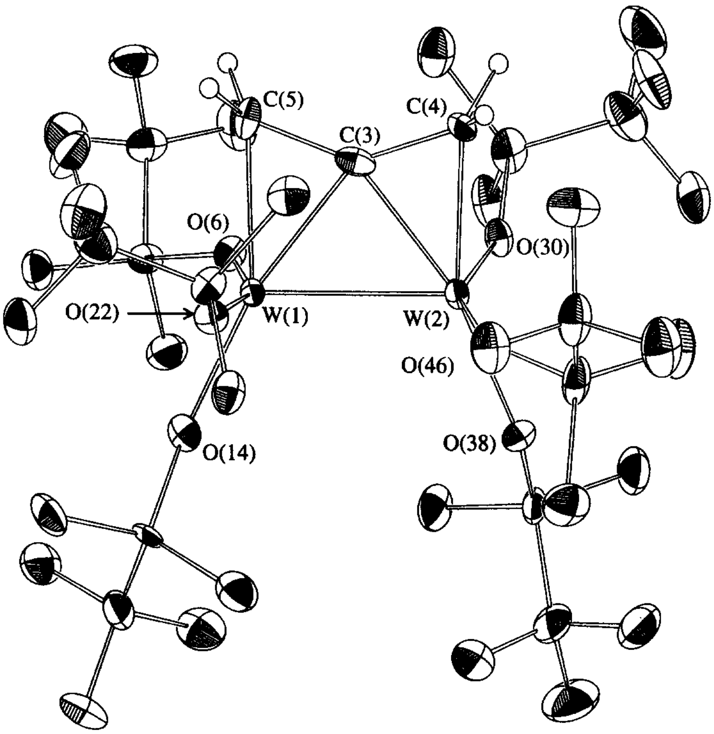

Fig. 5. An ORTEP drawing of the $W_2(OCMe_2CF_3)_6(\mu\text{-}CH_2CCH_2)$ molecule.

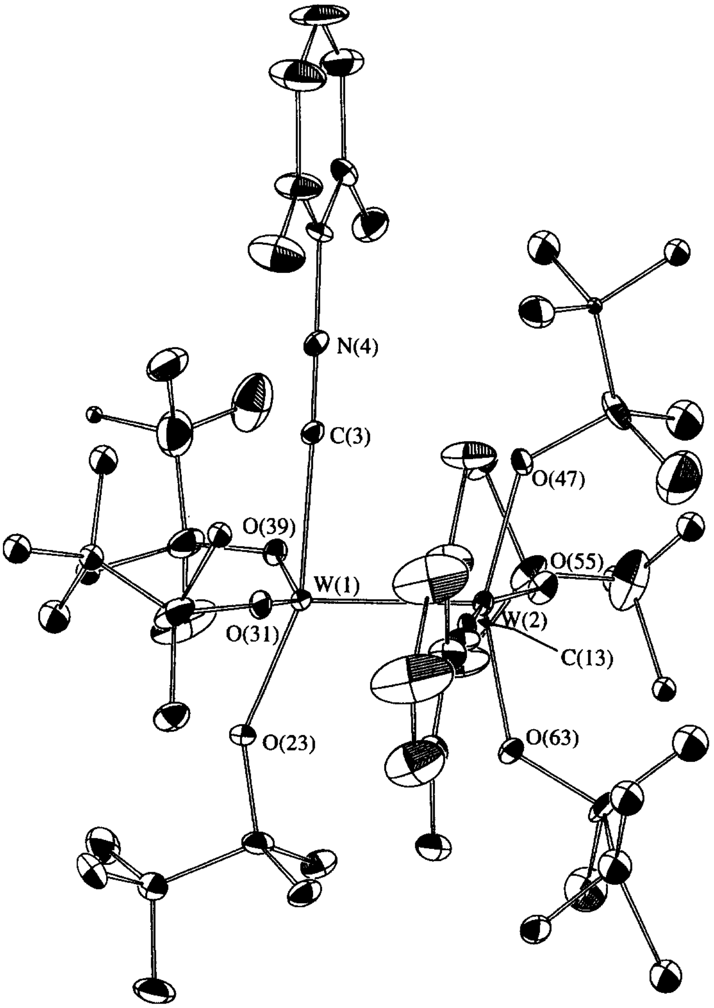

Fig. 6. An ORTEP drawing of the $W_2(OCMe_2CF_3)_6(CNxylyl)_2$ molecule.

Table 5. Selected bond distances (Å) and angles (°) for $W_2(OCMe_2CF_3)_6(NCxylyl)_2$

W(1)—W(2)	2.4427(6)
W(1)—O(23)	1.936(6)
W(1)—O(31)	1.933(6)
W(1)—O(39)	1.935(6)
W(1)—C(3)	2.152(9)
W(2)—O(47)	1.939(6)
W(2)—O(55)	1.937(6)
W(2)—O(63)	1.930(6)
W(2)—C(13)	2.143(10)
N(4)—C(3)	1.15(1)
N(14)—C(13)	1.160(1)

W(2)—W(1)—O(23)	113.1(2)
W(2)—W(1)—O(31)	100.3(2)
W(2)—W(1)—O(39)	106.2(2)
W(2)—W(1)—C(3)	86.3(2)
O(23)—W(1)—O(31)	92.3(3)
O(23)—W(1)—O(39)	91.9(3)
O(23)—W(1)—C(3)	160.5(3)
O(31)—W(1)—O(39)	149.0(3)
O(31)—W(1)—C(3)	82.6(3)
O(39)—W(1)—C(3)	83.3(3)
W(1)—W(2)—O(47)	101.6(2)
W(1)—W(2)—O(55)	114.1(2)
W(1)—W(2)—O(63)	105.0(2)
W(1)—W(2)—C(13)	84.3(2)
O(47)—W(2)—O(55)	92.2(3)
O(47)—W(2)—O(63)	148.3(3)
O(47)—W(2)—C(13)	82.1(3)
O(55)—W(2)—O(63)	92.3(3)
O(55)—W(2)—C(13)	161.6(3)
O(63)—W(2)—C(13)	83.8(3)
W(1)—O(23)—C(24)	147.9(6)
W(1)—O(31)—C(32)	133.1(7)
W(1)—O(39)—C(40)	141.5(8)
W(2)—O(47)—C(48)	131.2(6)
W(2)—O(55)—C(56)	148.1(6)
W(2)—O(63)—C(64)	134.1(6)
W(1)—C(3)—N(4)	178.0(8)
W(2)—C(13)—N(14)	176.5(8)

W—W—C angles are 83° (av.) and the dihedral angle between the two W—W—C planes is close to 90° which facilitates a mixing of W—W d_π and Wd_π—CNπ^* bonding as described for the dicarbonyl adduct previously [11]. A view looking down the M—M axis of the central $W_2O_6(CN)_2$ core is shown in Fig. 7.

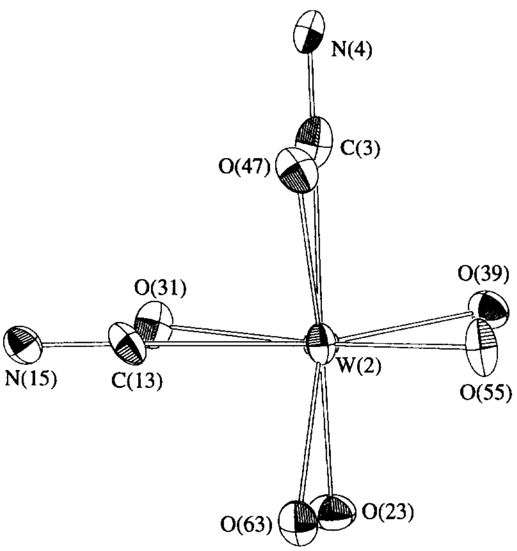

Fig. 7. A view of the central skeleton of the $W_2(OCMe_2CF_3)_6(CNxylyl)_2$ molecule looking down the M—M bond axis.

$W_2(OCMe(CF_3)_2)_4(NMe_2)_2(CNxylyl)_2$. An ORTEP diagram of the molecule showing the atom numbering scheme is given in Fig. 8. Selected bond distances and angles are given in Table 6. The molecular structure contrasts with that seen for the *bis*-isocyanide and *bis*-carbonyl adducts of $W_2(OCMe_2CF_3)_6$ in that the core is made up of two staggered four coordinate W atoms, where the C(47)—W(1)—W(2)—C(57) angle is 41.9°. The W—W distance of 2.380(1) Å is only slightly longer than that observed in $W_2(OCMe(CF_3)_2)_4(NMe_2)_2$ and significantly shorter than the W—W distances in the *bis*-carbonyl and *bis*-isocyanide adducts of $W_2(OCMe_2CF_3)_6$. The two W—W—C angles are 90.2(2)° and 88.6(2)°. The W—N distances of 1.93(1) Å (av.) and W—O distances of 2.00(2) Å (av.) are notably longer than in the parent compound $W_2(OCMe(CF_3)_2)_4(NMe_2)_2$ [12] which reflects the increase in coordination number at the metal center.

EXPERIMENTAL

General operating procedures for the manipulation of air-sensitive samples were observed.

Preparation of $[W_2(O^tBu)_6(py)_2]$. Pyridine (1 cm^3) was added to a solution of $W_2(O^tBu)_6$ [13] (153 mg, 0.190 mmol) in 10 cm^3 of dry, degassed benzene at 23°C. The solution was stirred at 23°C for 1 h and the solvent was reduced under vacuum. Crystallization in dry, degassed toluene at −20°C gave dark red microcrystals in 81% yield. The crystals obtained when using pyridine were not suitable for a single crystal X-ray study. The use of 4-Me-pyridine during the preparation did afford crystals (from hexanes) of $[W_2(O^tBu)_6(4\text{-Me-py})_2]$ (**1-Me**) suitable for study by X-ray analysis. ^1H NMR for **1** (300 MHz, C_7D_8, −30°C) $\delta = 8.43$ (br. multiplets, 2H), 6.85 (br. multiplets, 1H), 6.55 (br. multiplets, 2H), 2.40 (18H), 1.53 (18H), 1.20 (18H). ^1H NMR for **1** (300 MHz, C_7D_8, 16°C) $\delta = 1.59$ (54H). $^{13}C\{^1H\}$ NMR for **1** (75 MHz, C_7D_8, −30°C) $\delta = 151.3$, 135.0, 122.5 (NC_5H_5); 82.0, 76.4, 74.4 ($C(CH_3)$); 34.8, 33.4, 33.1 ($C(CH_3)$).

Preparation of $[W_2(OCMe_2CF_3)_6(py)_2]$. Pyridine (1 cm^3) was added to a solution of $W_2(OCMe_2CF_3)_6$ [4] (170 mg, 0.15 mmol) in 10 cm^3 of dry, degassed benzene at 23°C. The solution was stirred at 23°C for 1 h

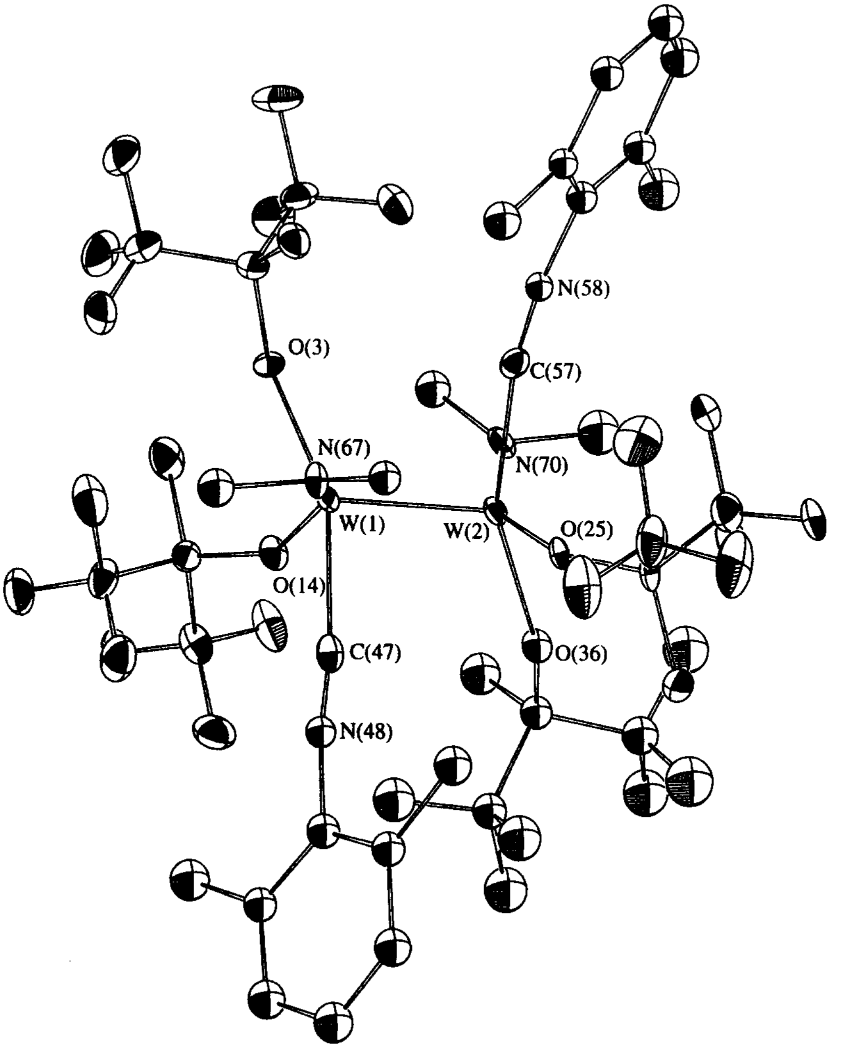

Fig. 8. An ORTEP drawing of the $W_2(OCMe(CF_3)_2)_4(NMe_2)_2(CNxylyl)_2$ molecule.

and the solvent was reduced under vacuum. Crystallization from dry, degassed benzene (65–23°C) gave X-ray quality black crystals in 68% yield. ^1H NMR (300 MHz, C_7D_8, −80°C) $\delta = 8.43$ (br. multiplets, 2H), 6.85 (br. multiplets, 1H), 6.55 (br. multiplets, 2H), 1.95 (6H), 1.50 (6H), 1.33 (6H), 1.31 (6H), 0.92 (6H), 0.86 (6H). $^{19}F\{^1H\}$ NMR (283 MHz, C_7D_8, 16°C, ext. ref. CF_3CO_2H $\delta = -78.45$) $\delta = -80.8$ (br. 12F), −82.2 (6F). $^{19}F\{^1H\}$ NMR (283 MHz, C_7D_8, −50°C, ext. ref. CF_3CO_2H $\delta = -78.45$) $\delta = -78.8$ (6F), −79.0 (6F), −80.1 (6H).

Preparation of $W_2(OCMe_2CF_3)_6(CN\text{-}2,6\text{-}Me_2C_6H_3)_2$. $W_2(OCMe_2CF_3)_6$ [4] (200 mg, 0.18 mmol) and xylylisocyanide (91 mg, 0.71 mmol) solids were added to a 30 cm^3 Schlenk flask in a nitrogen glove box. Hexanes (3 cm^3) were added and the solution was concentrated. Brown, tetragonal thin plates (199 mg, 81%) were obtained at −35°C. Recrystallization from Et_2O at −35°C yielded crystals for the X-ray study. ^1H NMR (300 MHz, C_7D_8, 23°C): δ 2.52 (s, 12H), 2.29 (s, 6H), 2.21 (s, 6H), 1.49 (s, 6H), 1.20 (s, 12H), 1.18 (s, 6H), 6.5–6.9 (br. multiplets 6H). $^{19}F\{^1H\}$ NMR (340 MHz, C_7D_8, 23°C): δ −75.9 (s, 6F), −76.2 (s, 6F), −84.4 (s, 6F).

Preparation of $W_2(OSi^tBuMe_2)_6(CN\text{-}2,6\text{-}Me_2C_6H_3)_2$. $W_2(OSi^tBuMe_2)_6$ [2] (25 mg, 0.022 mmol) and $CN\text{-}2,6\text{-}Me_2C_6H_3$ (34 mg, 0.22 mmol) were dissolved in 0.6 cm^3 of toluene-d_8 in an NMR tube. The kinetically labile **4** did not yield a crystalline compound. ^1H NMR (300 MHz, C_7D_8, −20°C): δ 6.6–7.1 (br, 6H), 2.0 (s, 12H), 1.16 (s, 18H), 1.06 (s, 18H), 0.943 (s, 18H), 0.34 (s, 6H), 0.33 (s, 6H), 0.26 (s, 18H), 0.24 (s, 6H).

Preparation of $W_2(OCMe(CF_3)_2)_4(NMe_2)_2(CN\text{-}2,6\text{-}Me_2C_6H_3)_2$. $W_2(OC(CF_3)_2Me)_4(NMe_2)_2$ [13] (150 mg, 0.13 mmol) and $CN\text{-}2,6\text{-}Me_2C_6H_3$ were combined in a 30 cm^3 Schlenk flask in a nitrogen glove box. THF (10 cm^3) was added to the flask followed by reduction in volume to concentrate the solution. Crystallization at −35°C gave bundles of deep red fibers which were separated by sublimation of excess isocyanide at 23°C to give 160 mg (85%). Recrystallization from CH_2Cl_2

Table 6. Selected bond distances (Å) and angles (°) for $W_2(NMe_2)_2(OCMe(CF_3)_2)_4(CNxylyl)_2$

W(1)—W(2)	2.3820(6)
W(1)—O(3)	2.003(5)
W(1)—O(14)	1.993(5)
W(1)—N(67)	1.933(6)
W(1)—C(47)	2.133(9)
W(2)—O(25)	2.018(5)
W(2)—O(36)	1.986(6)
W(2)—N(70)	1.926(7)
W(2)—C(57)	2.147(8)
C—F	1.34(1) (av.)
N(48)—C(47)	1.16(1)
N(58)—C(57)	1.42(1)

W(2)—W(1)—O(3)	114.8(2)
W(2)—W(1)—O(14)	102.4(2)
W(2)—W(1)—N(67)	104.5(2)
W(2)—W(1)—C(47)	88.6(2)
O(3)—W(1)—O(14)	87.2(2)
O(3)—W(1)—N(67)	95.4(3)
O(3)—W(1)—C(47)	156.4(3)
O(14)—W(1)—N(67)	149.0(3)
O(14)—W(1)—C(47)	84.4(3)
N(67)—W(1)—C(47)	80.9(3)
W(1)—W(2)—O(25)	108.4(2)
W(1)—W(2)—O(36)	113.3(2)
W(1)—W(2)—N(70)	99.3(2)
W(1)—W(2)—C(57)	90.2(2)
O(25)—W(2)—O(36)	84.0(2)
O(25)—W(2)—N(70)	149.5(3)
O(25)—W(2)—C(57)	80.7(3)
O(36)—W(2)—N(70)	96.80(26)
O(36)—W(2)—C(57)	155.1(3)
N(70)—W(2)—C(57)	86.7(3)
W(1)—O(3)—C(4)	143.8(5)
W(1)—O(14)—C(15)	140.2(5)
W(2)—O(25)—C(26)	139.3(5)
W(2)—O(36)—C(37)	145.2(5)
C(47)—N(48)—C(49)	173.0(8)
C(57)—N(58)—C(59)	172.3(8)
W(1)—N(67)—C(68)	134.6(5)
W(1)—N(67)—C(69)	114.1(5)

gave X-ray quality deep red cubes. ^{1}H NMR (300 MHz, C_7D_8, 80°C): δ 6.6–7.0 (br, 6H), 4.64 (s, 6H), 2.58 (s, 6H), 2.39 (s, 12H), 1.69 (s, 12H). ^{1}H NMR (300 MHz, C_7D_8, −40°C): δ 6.6–7.0 (br, 6H), 4.55 (s, 3H), 4.52 (s, 3H), 2.53 (s, 3H), 2.14 (s, 3H), 2.02 (s, 3H), 1.76 (s, 3H), 1.71 (s, 3H), 1.19 (s, 3H).

Preparation of $W_2(OCMe_2CF_3)_6(\mu,\eta^2,\eta^2\text{-}CH_2CCH_2)$. $W_2(OCMe_2CF_3)_6$ [4] (25 mg, 0.022 mmol) was dissolved in 0.6 cm^3 of C_7D_8 in an NMR tube equipped with a J. Young valve. Allene (10 equiv.) was transferred at −196°C to the NMR tube by means of a calibrated gas manifold. The reaction mixture was thawed and placed at −35°C for 24 h. Analysis by ^{1}H NMR spectroscopy at −20°C allows an estimated yield of 85% with the remaining tungsten containing compound being $W_2(OCMe_2CF_3)_6$. Addition of a large excess of allene (>20 equiv.) results in the formation of a transparent solid proposed to be polyallene. ^{1}H NMR (300 MHz, C_7D_8, −20°C): δ 1.66, 1.37, 1.04 (s, 12H), 7.57 (s, 4H). ^{13}C{^{1}H} NMR (75 MHz, C_7D_8, −20°C): δ 265.1, 95.0, 85.1 (q), 81.4 (q), 25.1 (s), 24.8 (s), 24.1 (s). ^{19}F{^{1}H} NMR (340 MHz, C_7D_8, −20°C): δ −80.4 (s, 6F), −81.0 (s, 12F).

Preparation of $W_2(OCMe_2CF_3)_6(\mu,\eta^2,\eta^2\text{-}4\text{-}Me\text{-}C_6H_4N{=}C{=}NC_6H_4\text{-}4\text{-}Me)$. $W_2(OCMe_2CF_3)_6$ [4] (275 mg, 0.244 mmol) 4-Me-C_6H_4-N=C=N-C_6H_4-4-Me (119 mg, 0.535 mmol) were combined in a 30 cm^3 Schlenk flask in a nitrogen atmosphere glove box. Hexanes (5 cm^3) were added to the Schlenk flask. Reduction of the volume followed by crystallization at −35°C afforded dark green cubes (280 mg, 85%) that were suitable for X-ray analysis. ^{1}H NMR (300 MHz, C_7D_8, 23°C): δ 6.99 (d, $^3J_{HH}$ = 32 Hz), 6.80 (d, $^3J_{HH}$ = 32 Hz), 1.85, 1.71, 1.46 (s, 12H). ^{19}F{^{1}H} NMR (340 MHz, C_7D_8, 23°C): δ −80.0 (s, 6F), −80.8 (s, 12F).

Single crystal X-ray crystallographic studies— General operating procedures and listings of programs have been previously given [14]. A summary of crystallographic data is given in Table 7. Complete listings of atomic coordinates have been deposited with the Cambridge Crystallographic Data Center.

CONCLUSIONS

The molecular structures of the pyridine, carbodiimide and allene adducts of $W_2(O^tBu)_6$ and $W_2(OCMe_2CF_3)_6$ are remarkably similar and belie the otherwise very different reactivities of the two complexes. This, of course, supports the view that structural data rarely provide much insight into reactivity. The relative thermal stability of the allene adduct reported here leads us to propose that the greater reactivity of the *t*-butoxide arises because the more basic ^{t}BuO ligand promotes an allene to propyne isomerization. That $W_2(OCMe_2CF_3)_6(\mu,\eta^2,\eta^2\text{-}CH_2CCH_2)$ does not react with additional allene to give a compound of the type $W_2(OR)_6(\mu,\eta^1,\eta^3\text{-}C_3H_4)(\eta^2\text{-}C_3H_4)$ as seen for R = ^{t}Bu may reflect the less easily oxidized and less π-basic W_2 core when supported by $(CF_3)Me_2CO$ ligands. This too may be the reason for the formation of the 2 : 1 isocyanide and carbonyl adducts with $W_2(OCMe_2CF_3)_6$ as compared to the $W_2(O^tBu)_6(\mu\text{-}L)$ compounds (L = CO, CNAr). The latter contain highly reduced C—O and C—N bonds as a result of extensive back-bonding from the W_2 *d*π electrons [8,9].

In the compound $W_2(OCMe(CF_3)_2)_4(NMe_2)_2$ which contains both strongly π-donating amide ligands and weakly π-donating $(CF_3)_2MeCO$ ligands the metal centers are sufficiently Lewis acidic to bind xylylisocyanide (2 equiv.). This contrasts with the behavior of $W_2(NMe_2)_6$ and testifies to the electronic

Table 7. Summary of crystal data

	I[a]	**II**[b]	**III**[c]	**IV**[d]	**V**[e]	**VI**[f]
Empirical formula	$C_{36}H_{68}N_2O_6W_2$	$C_{34}H_{46}F_{18}N_2O_6W_2$	$C_{27}H_{40}F_{18}O_6W_2$	$C_{39}H_{50}F_{18}N_2O_6W_2$; $1/2C_6H_{14}$	$C_{42}H_{54}F_{18}N_2O_6W_2$	$C_{38}H_{42}F_{24}N_4O_4W_2$
Color of crystal	Black	Black	Black	Black	Dark Brown	Red
Crystal dimensions (mm)	0.13 × 0.13 × 0.24	0.20 × 0.24 × 0.40	0.08 × 0.20 × 0.25	0.24 × 16 × 0.22	0.10 × 0.15 × 0.15	0.16 × 0.20 × 0.20
Space group	$C2/c$	$C2/c$	$P2_1/c$	$P\bar{1}$	$P\bar{1}$	$P\bar{1}$
Cell dimensions						
Temperature (°)	−160	−170	−165	−169	−171	−170
a (Å)	30.636(14)	23.733(6)	16.816(3)	14.634(3)	11.659(2)	11.101(2)
b (Å)	10.818(3)	10.458(2)	10.633(1)	15.408(3)	21.373(3)	21.323(3)
c (Å)	20.357(9)	20.396(4)	21.616(3)	12.428(2)	10.944(2)	10.666(1)
α (°)				113.27(1)	97.14(1)	94.87(1)
β (°)	143.58(1)	125.17(1)	102.71(1)	93.22(1)	114.78(1)	109.14(1)
γ (°)				81.34(1)	84.00(1)	95.43(1)
Z	4	4	4	2	2	2
V (Å^3)	4005.69	4138.24	3770.32	2545.02	2452.47	2356.07
Calculated Density (p, g cm^{-3})	1.646	2.049	2.062	1.821	1.886	2.033
Wavelength (Å)	0.71069	0.71069	0.71069	0.71069	0.71069	0.71069
Molecular Weight	992.64	1276.32	1170.28	1395.59	1392.57	1442.44
Linear Absorption Coefficient (cm^{-1})	59.032	57.970	63.512	47.208	48.988	51.184
Detector to sample distance (cm)	22.5	22.5	22.5	22.5	22.5	22.5
Sample to source distance (cm)	23.5	23.5	23.5	23.5	23.5	23.5
average ω scan width at half height (deg)	0.25	0.25	0.25	0.25	0.25	0.25
scan speed (deg/min)	5.0	8.0	8.0	6.0	6.0	8.0
scan width (deg + dispersion)	1.8	2.0	2.0	2.0	2.0	2.0
individual background (s)	10	4	4	6	6	4
aperature size (mm)	3.0 × 4.0	3.0 × 4.0	3.0 × 4.0	3.0 × 4.0	3.0 × 4.0	3.0 × 4.0
2θ range (deg)	6–50	6–55	6–45	6–45	6–45	6–45
Total no. of reflections collected	7601	10195	7566	9685	8550	10037
no. of unique intensities	3543	4778	4946	6686	6442	6164
no. with F > 0.00	3405	4527	4580	6237	6122	5847
no. with F > σ(F)	3308					
no. with F > 2.33σ(F)	3158					
no. with F > 3*σ(F)		4150	4169	5770	5745	5440
$R(F)$	0.0309	0.0470	0.0366	0.0564	0.0422	0.0363
$Rw(F)$	0.0332	0.0492	0.0362	0.0548	0.0452	0.0375
goodness of fit for last cycle	0.985	1.288	1.156	1.661	1.533	1.145
maximum δ/σ for last cycle	0.05	0.002	0.23	0.02	0.27	0.035

[a] **I** = $W_2(O^tBu)_6(4\text{-Mepy})_2$.
[b] **II** = $W_2(OCMe_2CF_3)_2(py)_2$.
[c] **III** = $W_2(OCMe_2CF_3)_6(\mu\text{-}CH_2CCH_2)$.
[d] **IV** = $W_2(OCMe_2CF_3)_6(\mu\text{-CN-}p\text{-tolyl})_2$.
[e] **V** = $W_2(OCMe_2CF_3)_6(\text{CNxylyl})_2$.
[f] **IV** = $W_2(NMe_2)(OCMe(CF_3)_2)_6(\text{CNxylyl})_2$.

influence of the $OCMe(CF_3)_2$ ligands at the ditungsten center.

Obviously the results reported here merely add to our knowledge of the chemistry of $W_2(OR)_6$ compounds but do not provide quantitative information concerning the factors influencing the vastly different reactivity seen toward certain substrates such as $MeC{\equiv}N$. However, more quantitative studies are underway.

Acknowledgements—We thank the National Science Foundation for support and D.B.T. thanks General Electric for a fellowship.

REFERENCES

1. Chisholm, M. H., Cotton, F. A., Extine, M. W. and Kelly, R. L., *Inorg. Chem.*, 1979, **18,** 116.
2. Chisholm, M. H., Cook, C. M. and Streib, W. E., *Inorganica Chim. Acta*, 1992, **198–200,** 63.
3. Schrock, R. R., Listemann, M. L. and Sturgeoff, L. G., *J. Am. Chem. Soc.*, 1982, **104,** 4291.
4. Freudenberger, J. H., Pedersen, S. F. and Schrock, R. R., *Bull. Soc. Chim. France*, 1985, 349.
5. Budzichowski, T. A., Chisholm, M. H. and Folting, K., *Chem.—A Eur. J.*, 1996, **2,** 110.
6. (a) μ-allene: Cayton, R. H., Chacon, S. J., Chisholm, M. H., Hampden-Smith, M. J., Huffman, J. C., Folting, K., Ellis, P. D. and Huggins, B. A., *Angew. Chem. Int. Ed. Engl.*, 1989, **28,** 1523; Chacon, S. T., Chisholm, M. H., Hampden-Smith, M. J., Huffman, J. C. and Folting, K., *Organometallics*, 1991, **10,** 3722; (b) 1,3-di-*p*-tolyl-carbodiimide: Cotton, F. A., Schwotzer, W. and Shamshoum, E. S., *Organometallics*, 1985, **4,** 461.
7. Chisholm, M. H., Folting, K., Hoffman, D. M. and Huffman, J. C., *J. Am. Chem. Soc.*, 1984, **106,** 6794.
8. Chisholm, M. H., Clark, D. L., Ho, D. and Huffman, J. C., *Organometallics*, 1987, **6,** 1532.
9. Chisholm, M. H., Hoffman, D. M. and Huffman, J. C., *Organometallics*, 1985, **4,** 987 and refs therein.
10. Appleton, T. G., Clark, H. C. and Manzer, L. E., *Coord. Chem. Rev.*, 1973, **10,** 352.
11. Budzichowski, T. A., Chisholm, M. H., Tiedtke, D. B., Huffman, J. C. and Streib, W. E., *Organometallics*, 1995, **14,** 2318.
12. For the preparation and structure see this issue of *Polyhedron.*
13. Akiyama, M., Chisholm, M. H., Cotton, F. A., Extine, M. W., Haitko, D. A., Little, D. and Fanwick, P. E., *Inorg. Chem.*, 1979, **18,** 2321.
14. Chisholm, M. H., Folting, K., Huffman, J. C. and Kirkpatrick, C. C., *Inorg. Chem.*, 1984, **23,** 1021.